

## Microsolvation of HCl within Cold NH<sub>3</sub> Clusters

Paweł Siuda,<sup>†,‡</sup> Nevin Uras-Aytemiz,<sup>†</sup> and Joanna Sadlej<sup>\*,‡</sup>

Department of Chemistry, Suleyman Demirel University, 32260 Isparta, Turkey, and Department of Chemistry, University of Warsaw, Pasteur 1, 02-093 Warsaw, Poland

Received: March 28, 2008; Revised Manuscript Received: August 7, 2008

The solid state solvation of HCl molecules with small ammonia clusters at an average temperature of 100 K was investigated by on-the-fly molecular dynamics methodology. Structures close to the proton jump from HCl molecule to the ammonia have been further checked with the MP2/aug-cc-pvDZ calculations. Ionization of HCl and/or sharing of the proton were found. Two Zundel-type ions were observed—one with proton being shared between ammonium ion and Cl<sup>−</sup> anion (Cl<sup>−</sup>⋯H<sup>+</sup>⋯NH<sub>3</sub>) in all complexes, and the second, between hydrogen chloride and Cl<sup>−</sup> anion in the HCl⋯Cl<sup>−</sup>⋯NH<sub>4</sub><sup>+</sup>⋯(NH<sub>3</sub>)<sub>2</sub> complex. However, in contrast to methanol clusters, ammonia clusters are not good for the proton wires since once the proton moves to ammonia, it is localized on the ammonium ion units.

### 1. Introduction

The interaction of hydrogen chloride and ammonia serve as a model of acid–base pair for a study of proton-transfer reactions, which is a crucial problem in molecular biology. This reaction is instantaneous in the aqueous solution, and the well-established product is the ion pair NH<sub>4</sub><sup>+</sup>Cl<sup>−</sup>, resulting from the transfer of a proton from HCl to NH<sub>3</sub>. This is an example of strong acid–base reaction in general chemistry.

The questions about a detailed mechanism of proton transfer and the stable form of ClH⋯NH<sub>3</sub> dimer in the gas-phase have been receiving considerable attention for many years. Microwave experiments by Howard and Legon<sup>1,2</sup> revealed that the system exists as a hydrogen-bonded complex with HCl as the hydrogen bond donor and the ammonia as the acceptor molecule rather than an ion pair. Matrix-isolation studies in solid neon and argon supported the hydrogen-bonded complex ClH⋯NH<sub>3</sub><sup>3,4</sup> without substantial proton transfer. These experimental data are supported by several ab initio calculations.<sup>5,6</sup>

Water molecule can play a crucial role in proton transfer in the ClH⋯NH<sub>3</sub> system. The effect of the addition of water molecule to the complex has been studied by ab initio calculations.<sup>5–13</sup> It was found that two water molecules attached to the complex are enough to stabilize the ion-pair structure.<sup>5,6</sup> Thus, ionic ammonium chloride can be produced in the gas phase in the presence of water vapor.<sup>11</sup>

Much less attention was devoted to acid solvation at solid phase. In contrast to liquid phase, solid-phase solvation accompanies the formation of well-defined crystal structures. Such mixed acid–solvent crystals give opportunities to investigate well-defined structures and different environments.

Study of the clusters of molecules opens an exciting possibility for exploring the structural transition from the molecular structures to the defined solvating environments and to probe the induced extent of proton transfer. Thus, clusters can be considered as a bridge between the gas and the condensed phases; therefore, during the past years, the study of clusters has become an important branch of research.

Recently, HCl solvation on ice nanoparticles has been studied by comparative experimental IR spectroscopy and computational modeling.<sup>14–17</sup> It was found that solvation and ionization of hydrogen chloride have been dependent on its coverage and temperature. At low temperatures and low surface coverage, HCl has adsorbed molecularly on ice nanoparticles, while the contact ion pairs H<sub>3</sub>O<sup>+</sup>Cl<sup>−</sup> were found at higher concentration of HCl or higher temperatures. The final step in the solvation mechanism was the proton transfer among the water molecules.

A similar series of studies have addressed the issue of solid-state solvation of HX (X = Cl, Br) in different H-bonded systems containing oxygen clusters such as methanol (CH<sub>3</sub>OH),<sup>18</sup> and dimethyl ether (DME, (CH<sub>3</sub>)<sub>2</sub>O).<sup>18</sup> These systems were investigated in a series of studies of FTIR spectroscopy combined with different molecular modeling techniques. In these studies, HCl solvation and ionization have been questioned in terms of HCl coordination on the surface and the number of “solvent” molecules. In contrast to the ice surface, which includes both dangling-O and dangling-H sites to the acidic adsorbate molecules, the methanol surface contains only dangling-O sites. Thus, adsorbate HCl has attached via a single H-bond to the dangling-O at low temperatures. However, some of the acid adsorbate molecules manage to break into the H-bonded chains of methanol within the surface. Presence of such a two-coordinated HCl band was identified at ca. 1700 cm<sup>−1</sup>. Three H-bonds to a HCl molecule to induce acid ionization was proposed as a requirement. Moreover, it was shown that the proton delocalized around the ring cluster of methanol, forming methoxonium ions on the time scale of several picoseconds.<sup>19,20</sup> The IR spectra computed with on-the-fly molecular dynamics for the clusters display broad bands assignable to specific proton states as well as the continuum showing the fluxional nature of the proton. This was the evidence for the proton wires along the methanol clusters.

All of this information forms the basis for the study that examines HCl solvation and ionization in other H-bonded system. This study is an extension of previous investigations of acid hydrates. Now the aim is to investigate the microsolvation of HCl with the cold ammonia clusters.

There are few published computational studies of the (NH<sub>3</sub>)<sub>m</sub>⋯(HCl)<sub>n</sub> clusters.<sup>6,21,22</sup> The most comprehensive study on ammonia–hydrogen chloride clusters to date is the work of

\* To whom correspondence should be addressed. Fax: +48 22 822-59-96. E-mail: sadlej@chem.uw.edu.pl.

<sup>†</sup> Suleyman Demirel University.

<sup>‡</sup> University of Warsaw.

Bacelo and Fioressi for  $(\text{NH}_3)_m \cdots \text{HCl}$ ,  $m = 1-4$ , studied by ab initio Monte Carlo (MC) simulated annealing with a combination of different levels of quantum mechanical calculations (i.e., density functional theory (DFT) and MP2).<sup>21</sup> The ab initio MC simulations were used to identify the minimum energy structures in which both ionic and molecular HCl were found for larger clusters. They also reported harmonic frequencies that associates each isomer obtained from ab initio MC simulations.<sup>21</sup>

Significant differences can be noted between the ammonia and water clusters with HCl molecule. The ammonia is a much stronger base for hydrochloric acid than water since nitrogen has the highest known proton affinity. The basic structure unit of the model clusters was a ring of ammonia molecules with HCl either inserted into the ring or adsorbed onto the ring. Therefore, clusters  $(\text{NH}_3)_m \cdots (\text{HCl})_n$ ,  $m = 1-4$ ,  $n = 1, 2$ , serve as a good model of acid–base interactions.

Atomic level understanding of this system is a challenging problem. Simulations are difficult because of the lack of empirical potentials that could include the description of the potential proton transfer from acid to ammonia. Therefore, in the first step of our paper, the computational study employing on-the-fly Car–Parrinello molecular dynamics (MD) method was carried out to observe the mechanism and determine structural requirements for the ionization process of HCl. This technique enables simulation of the dynamics and the spectra of these anharmonic proton-transfer systems. Moreover, the different solvation states can be taken into account, as well as the delocalization, and the proton transfer can be studied in a time-dependent scheme. To double check on-the-fly results, in the second step, ab initio supermolecular calculations were carried out for the clusters close to the proton jump from HCl molecule to ammonia.

Interpretations of the spectra for this very anharmonic system also possess considerable difficulties. The complex issue could be proton dynamics, and the protonated ammonia could appear in the form of Zundel type  $\text{Cl}^- \cdots \text{H}^+ \cdots \text{NH}_3$  ion.<sup>23</sup> Therefore, we also reported the infrared spectra obtained from on-the-fly dipole–dipole correlation functions for these systems. Our study differs from the work of Bacelo and Fioressi.<sup>21</sup> On-the-fly study enables investigation of cluster dynamics in addition to minima. Our aim is thus 2-fold: first, to investigate dynamics of the system for a given minimum at low temperatures and, second, to calculate accompanying infrared spectra for these highly anharmonic systems. Therefore, this study might be a base for future experimental work.

## 2. Computational Methods

**2.1. Ab Initio Molecular Dynamics Simulations.** A number of  $(\text{NH}_3)_m \cdots (\text{HCl})_n$  ( $m = 1-4$ ,  $n = 1-2$ ) trajectory calculations was carried out using ab initio molecular dynamics as implemented in the electronic structure code QUICKSTEP,<sup>24</sup> which is part of the CP2K package.<sup>25</sup> It employs the Gaussian plane wave method, which is based on the Kohn–Sham formulation of DFT, and the exchange–correlation functional of Becke, Lee, Yang, and Parr (BLYP) were used.<sup>26</sup> The Kohn–Sham orbitals are expanded using a linear combination of atom-centered Gaussian-type orbital functions. The electronic charge density was described using an auxiliary basis set of plane waves. A Gaussian valence basis set of quadruple- $\zeta$  quality was augmented by three sets of polarization functions (QZV3P). Energies and forces from on-the-fly ab initio molecular dynamics simulation sampling of the Born–Oppenheimer surface were calculated for each MD step using the atomic pseudopotentials of the Goedecker, Teter, and Hutter type.<sup>27</sup> These clusters

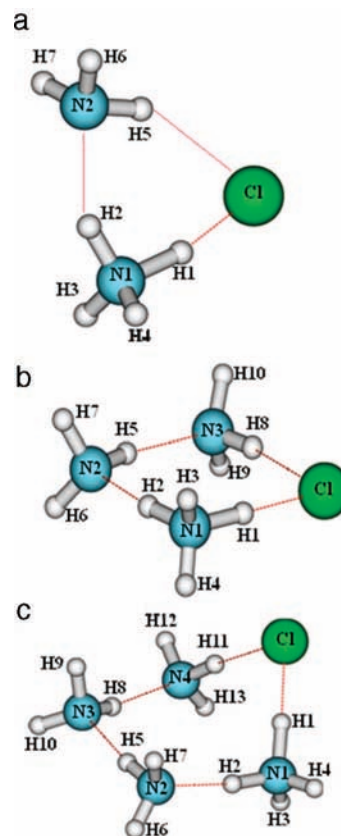


**Figure 1.** Structures of the  $\text{HCl} \cdots (\text{NH}_3)_m$ ,  $m = 2-4$  complexes: (a)  $\text{Cl}^- \cdots \text{NH}_4^+ \cdots \text{NH}_3$ ; (b)  $\text{Cl}^- \cdots \text{NH}_4^+ \cdots (\text{NH}_3)_2$ ; (c)  $\text{Cl}^- \cdots \text{NH}_4^+ \cdots (\text{NH}_3)_3$ .

represent solid phase because the heavy atoms are almost not changing their positions.

We have considered several different possible arrangements of clusters that can be adopted as a consequence of the donor/acceptor capacity of the subunits. The clusters,  $(\text{NH}_3)_m \cdots (\text{HCl})_n$  ( $m = 1-4$ ,  $n = 1-2$ ), constructed in this way are presented in Figure 1 and Figure 2. Each system has been subjected to a minimization procedure by using QUICKSTEP before constant energy MD simulations were performed. The time scale for each system and the average simulation temperature will be given in the related results part. The cluster spectra were obtained from the Fourier transform of the dipole–dipole correlation function as described in ref 28. This methodology was successfully applied in the past for the other condensed-phase systems.<sup>29-31</sup>

**2.2. Details of ab Initio Supermolecular Calculations.** The structures shown at Figure 1 and Figure 2 have been also subject to ab initio calculations at the MP2/aug-cc-pvDZ<sup>32</sup> level of theory to check and refine on-the-fly simulation results. The MP2 method was judged to be more suitable to the current problem than the commonly employed and cheaper DFT/B3LYP, because the latter tends to overestimate the tendency of HCl to stretch and ionize. This conclusion was reached from a comparison of MP2 and DFT results for the solvation of HCl in water molecules.<sup>15</sup> The optimal geometries and the frequency calculations at the same level were performed in order to confirm that the stationary points obtained from the gradient calculations correspond to minima. Our main objective was to calculate HCl bond lengths and frequencies for minima associated with different coordinations/structures.

The binding energies of the complexes,  $E_{\text{bin}}$ , are defined as the difference between the energy of the cluster and those of

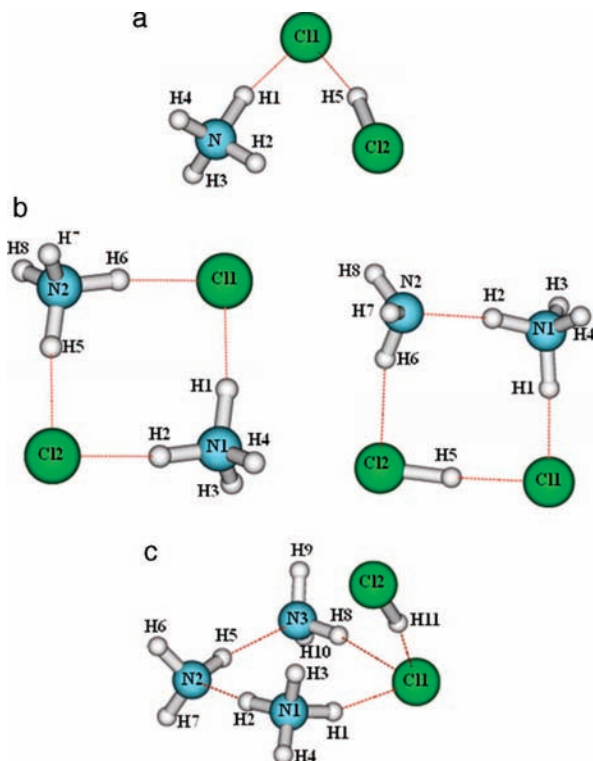


**Figure 2.** Structures of the  $(\text{HCl})_2 \cdots (\text{NH}_3)_m$ ,  $m = 1-3$  complexes: (a)  $\text{HCl} \cdots \text{Cl}^- \cdots \text{NH}_4^+$ ; (b)  $\text{Cl}^- \cdots \text{NH}_4^+ \cdots \text{Cl}^- \cdots \text{NH}_4^+$ ; (c)  $\text{HCl} \cdots \text{Cl}^- \cdots \text{NH}_4^+ \cdots (\text{NH}_3)_2$ .

the individual molecules in isolation (i.e., the interaction energy), corrected for basis set superposition error (BSSE), due to the deficiencies of a finite basis set, by using counterpoise procedure (CP).<sup>33</sup> The binding energies have been corrected also for the deformation error  $E_{\text{def}}$  that is the energy needed to deform the monomers from their optimal equilibrium geometries to their geometries in the complex. This contribution is always repulsive. Finally, the dissociation energies  $D_0$  are calculated from the binding energies by adding the difference of the zero-point energies ( $\Delta\text{ZPE}$ ) obtained from the MP2 level within the harmonic approximation. Ab initio calculations were carried out with the GAMESS program.<sup>34</sup>

The MP2/aug-cc-pvDZ HCl bond length and fundamental harmonic frequency were calculated as 1.283 Å and 3036 cm<sup>-1</sup>, as compared to experimental values of 1.275 Å, and 2991 cm<sup>-1</sup>, respectively.<sup>35</sup> Ammonia has an intensive band at 1045 cm<sup>-1</sup>, which corresponds to an umbrella-like bending mode. The second one, degenerated, is 1649 cm<sup>-1</sup> connected with the bending mode, and two stretching modes are 3481 and 3635 cm<sup>-1</sup>. The experimental spectra of the solid phase of ammonia at 100 K were reported.<sup>36</sup> The crystals gave a peak at 1057 cm<sup>-1</sup> for the umbrella-like bending, 1650 cm<sup>-1</sup> for bending and 3210 and 3375 cm<sup>-1</sup> for stretching modes.<sup>36</sup>

### 3. Computational Results and Discussion

**3.1. Structures of the Clusters: Results of the Molecular Dynamics.** The clusters subjected to this study are categorized by the number of HCl. Figure 1 presents the clusters with one HCl molecule,  $(\text{NH}_3)_m \cdots \text{HCl}$ ,  $m = 2-4$ , while Figure 2, the clusters  $(\text{NH}_3)_m \cdots (\text{HCl})_2$ ,  $m = 1-3$ , which are the results of ab initio MD, as described below. All the clusters contain an ionized form of HCl.

**One HCl Molecule Adsorbed on  $(\text{NH}_3)_2$ ,  $(\text{NH}_3)_3$ , and  $(\text{NH}_3)_4$  clusters.** The Quickstep optimized structures are shown in Figure 1a–c. These structures represent a miniature model of HCl

adsorbed on a cold ammonia nanoparticle surface. The model nanoparticle includes a simple ring of two, three, and four ammonia molecules. Condensed ammonia is known to be dominated by chains and rings of two-coordinated molecules,<sup>36,37</sup> so the present model may be a not-unreasonable representation of a portion of the nanoparticle system.

In all structures shown in Figure 1a–c, HCl was placed in three- and four-member NH<sub>3</sub> rings. On the other hand, some of the HCl on NH<sub>3</sub> rings as obtained by Bacelo and Fioressi<sup>21</sup> were also investigated (not shown). However, during the trajectory run, these structures turned out to be the structures shown in Figure 1a–c. Therefore, only these structures are discussed below.

**$\text{HCl} \cdots (\text{NH}_3)_2$  Cluster.** The dimer of  $\text{HCl} \cdots \text{NH}_3$  is a molecular complex.<sup>6,22</sup> However, inclusion of small molecules in the ammonia dimer, i.e., H<sub>2</sub>O, HCl, NH<sub>3</sub>, and CH<sub>3</sub>OH,<sup>8,38</sup> promotes the proton transfer from HCl to NH<sub>3</sub>. Our optimized structure from Quickstep gave also ionized HCl (see Figure 1a). The trajectory for this cluster run for 4 ps at an average temperature of 100 K. Although the optimized structure gives ionic HCl during the run, the acid proton undergoes large amplitude fluctuations between Cl and N. The mean N1–H1 and H1 $\cdots$ Cl distances, averaged over the trajectory, are 1.255 Å with standard deviation (SD) = 0.329 Å and 1.644 Å (SD = 0.312 Å), respectively (the corresponding MP2 level bond distances for N1–H1 and H1 $\cdots$ Cl are 1.150 and 1.714 Å, respectively). The N1H1 bond length in this proton sharing state is slightly larger than that with respect to ammonium cation (see below).

The similar localized proton sharing was observed when methanol molecule was added to the  $\text{HCl} \cdots \text{NH}_3$  complex: that is, the proton is not confined on NH<sub>3</sub>; rather, it is shared between N and Cl in the ternary complex of  $\text{HCl} \cdots \text{NH}_3 \cdots \text{CH}_3\text{OH}$ .<sup>38</sup> The cooperativity effect in the complex might be the reason for such behavior.

The average free NH bonds (i.e., N1H3 and N1H4) are 1.023 Å (SD = 0.071 Å and MP2 value is 1.019 Å) and the NH bond that has coordination to the other NH<sub>3</sub> is 1.052 Å (SD = 0.112 and 1.046 Å obtained at the MP2 level). The average free NH bond lengths of the other NH<sub>3</sub> molecule (N2H6 and N2H7) are similar to the one explained above (i.e., 1.023 Å (SD = 0.074 Å)). The NH bond length connected to Cl<sup>-</sup> from the other side is 0.01 Å longer than the free ones (N2H5 = 1.033 Å with SD = 0.101 Å). Roughly, 0.01 Å elongation was obtained at MP2 level (see Table SM1 of the Supporting Information). This might indicate that the presence of a very strong hydrogen bond of ammonium cation to Cl<sup>-</sup> on one side reduces the strength of the hydrogen bond to ammonia on the other side. A similar trend was observed for methanol wire containing a HCl molecule.<sup>18</sup>

**$\text{HCl} \cdots (\text{NH}_3)_3$  Cluster.** Addition of one NH<sub>3</sub> molecule to the  $\text{HCl} \cdots (\text{NH}_3)_2$  ring stabilizes the acid proton on the NH<sub>3</sub> molecule. Therefore, the structure contains the contact ion pair of NH<sub>4</sub><sup>+</sup> and Cl<sup>-</sup> and the rest of the NH<sub>3</sub> molecules solvate this ion, as shown in Figure 1b. The trajectory was run for 4 ps, and the average temperature was 100 K. During the trajectory, the proton coming from the HCl molecule localized on the ammonium cation, the average N1–H1 distance is 1.164 Å (SD = 0.176 Å), and the corresponding MP2 level distance is 1.125 Å. The distance of the other N–H bond that has a coordination with ammonia molecule is 1.071 Å (SD = 0.154 Å and MP2 gives 1.055 Å). The free H's of the ammonium cation have bond distances of 1.025 Å (SD = 0.073 Å), and the corresponding MP2 level distances are 1.018 Å.

**TABLE 1: Binding Energy, Zero-Point Correction, Deformation Error, and Dissociation Energy (kcal/mol) Calculated for Complexes  $\text{HCl}\cdots(\text{NH}_3)_m$ ,  $m = 2-4$ , and  $(\text{HCl})_2\cdots(\text{NH}_3)_m$ ,  $m = 1-3$ , at the MP2/aug-cc-pvDZ Level**

system	$E_{\text{int}}$	$\Delta\text{ZPE}$	$E_{\text{def}}$	$D_0$	with respect to
$\text{Cl}^-\cdots\text{NH}_4^+\cdots\text{NH}_3$	-55.1	5.9	35.7	-13.5	$\text{HCl} + 2\text{NH}_3$
$\text{Cl}^-\cdots\text{NH}_4^+\cdots(\text{NH}_3)_2$	-69.0	8.1	39.6	-21.3	$\text{HCl} + 3\text{NH}_3$
$\text{Cl}^-\cdots\text{NH}_4^+\cdots(\text{NH}_3)_3$	-101.3	11.1	58.7	-31.4	$\text{HCl} + 4\text{NH}_3$
$\text{HCl}\cdots\text{Cl}^-\cdots\text{NH}_4^+$	-54.8	5.2	36.8	-12.8	$2\text{HCl} + \text{NH}_3$
$(\text{Cl}^-\cdots\text{NH}_4^+)_2$	-170.2	11.3	123.2	-35.7	$2\text{HCl} + 2\text{NH}_3$
$\text{HCl}\cdots\text{Cl}^-\cdots\text{NH}_4^+\cdots\text{NH}_3$	-81.7	7.8	50.3	-23.7	$2\text{HCl} + 2\text{NH}_3$
$\text{HCl}\cdots\text{Cl}^-\cdots\text{NH}_4^+\cdots(\text{NH}_3)_2$	-110.3	10.4	66.0	-33.9	$2\text{HCl} + 3\text{NH}_3$

The N–H distance of the N2H5H6H7 molecule connected to the next of ammonia (i.e., N2–H5) is 0.005 Å longer than that connected to  $\text{Cl}^-$  (i.e., N3–H8, 1.039 Å (SD = 0.094 Å) versus 1.034 Å (SD = 0.087 Å), respectively), and the same trend was observed in MP2 level values (see Table 2). The rest of the N–H distances having no coordination (i.e., N2–H6, N2–H7, N3–H9, and N3–H10) were 1.025 Å.

**$\text{HCl}\cdots(\text{NH}_3)_4$  Cluster.** The pentamer  $\text{HCl}\cdots(\text{NH}_3)_4$  shown in Figure 1c is the biggest system studied by us, and it has also one of the most interesting trajectories. It was run for 4 ps. During the dynamics procedure, there was a transition at 2300 fs from a five-member ring to a four-member one with ammonium ion forming three hydrogen bonds: two with ammonia and one with chlorine anion. The snapshots from this trajectory are shown in Figure 3. Two ammonia molecules in the ring are both a single hydrogen bond donor and a single acceptor, while the third ammonia (whose nitrogen is labeled as N4), out of the ring, is only one hydrogen bond donor ( $t = 4000$  fs). Such a rearrangement might be explained in terms of the saturation of ammonium ion coordination. The extraction of one ammonia molecule from the ring driven by the ammonium ion in the trajectory might be proof for this explanation. It should be interesting to note at this point that structural transformation accompanies potential energy change. Since we are running constant energy molecular dynamics simulations, a drop in the potential energy causes a rise in the kinetic energy.

**Two HCl Molecules Adsorbed on  $\text{NH}_3$ ,  $(\text{NH}_3)_2$ ,  $(\text{NH}_3)_3$  Clusters (Figure 2a–c).** In these clusters extra acid solvation is provided by an additional hydrogen bond to HCl.

**$(\text{HCl})_2\cdots\text{NH}_3$  Cluster.** Addition of one HCl molecule to  $\text{HCl}\cdots\text{NH}_3$  dimer also catalyzes the proton transfer from HCl to  $\text{NH}_3$  molecule, as was reported by Li et al.<sup>8</sup> Both of our Quickstep and MP2 calculations also give the ionic structure shown in Figure 2a. However, as observed in the  $\text{HCl}\cdots(\text{NH}_3)_2$  cluster, the proton is not localized on the HCl molecule; rather it is shared between Cl and N atoms during the trajectory run of 4 ps at an average temperature of 106 K. The plot shown in Figure 4 gives a time evolution of the bond distances at the  $(\text{HCl})_2\cdots\text{NH}_3$ . In addition to this, the proton of HCl (H5–Cl2) makes excursion toward the other  $\text{Cl}^-$  ion, and this proton (H5) is shared between Cl1 and Cl2 atoms. This happens when the H1 proton is on the  $\text{NH}_3$  molecule that forms  $\text{NH}_4^+$ . In other words, the ammonium cation not the  $\text{NH}_3$  molecule catalyzes the proton transfer from the H5–Cl2 molecule to the Cl1<sup>-</sup> ion. During the trajectory, the mean H1Cl1 bond length was 1.583 Å (SD = 0.358 Å) and the H5Cl2 bond length was 1.343 Å (SD = 0.187 Å). The corresponding MP2 values were 1.720 and 1.344 Å, respectively. The average NH bond lengths were 1.332 Å (SD = 0.361 Å) for NH1, 1.027 Å (SD = 0.080 Å) for NH2, 1.027 Å (SD = 0.092 Å) for NH3, and 1.027 Å (SD = 0.092 Å) for NH4, while the corresponding MP2 optimized values are 1.145, 1.027, 1.021, and 1.020 Å, respectively.

**$(\text{HCl})_2\cdots(\text{NH}_3)_2$  Clusters.** There are two structures considered; one has the acid–ammonia–acid–ammonia and the other has acid–acid–ammonia–ammonia pattern. The Quickstep optimized structures are shown in Figure 2b,b', respectively.

In contrast to the water case  $\text{HCl}\cdots\text{HOH}\cdots\text{HCl}\cdots\text{HOH}$  the  $(\text{NH}_3)_2\cdots(\text{HCl})_2$  cluster shown in Figure 2b was found to be ionic by Tao et al. for a first time<sup>6</sup> and by Chaban et al.<sup>22</sup> This is understandable, since the proton affinity of ammonia is higher than that of water. Our Quickstep and MP2/aug-cc-pvDZ level calculations confirm the ionic structure. The trajectory was run for 4 ps at an average 99 K. During the run, the proton is localized on ammonium cations. The mean N–H bond lengths connecting to  $\text{Cl}^-$  were 1.088 Å (SD = 0.107 Å), and the free N–H ones were 1.026 Å (SD = 0.080 Å). The corresponding MP2 level bond lengths were calculated as 1.067 and 1.020 Å, respectively.

The structure shown in Figure 2b' has one ionic and one molecular HCl, and as far as is known by the authors, it has not been reported before. The trajectory was run for 4 ps at an average temperature of 104 K, and it was a very interesting trajectory.

The structures shown in Figure 1b and Figure 2a' are similar except that in one case HCl from the Cl side is solvated by ammonia (Figure 1b) and in the other case HCl is solvated by an extra HCl which also promotes ionization of the hydrogen chloride molecule. The  $\text{HCl}\cdots\text{HCl}$  self-solvation was reported before for HCl/water and HCl/methanol systems.<sup>15,18,19</sup> There are also differences between the two cases when the trajectories are concerned. When the structure shown in Figure 1b was subject to MD simulation, the ring structure was conserved during the run. On the other hand, the ring from the  $\text{H}_2\text{NH}\cdots\text{HCl}$  (i.e., N2H6 $\cdots$ H5Cl2, Figure 2b') side is broken up after 0.5 ps. Snapshots from a 4 ps trajectory of the cluster run at 104 K average temperature are shown in Figure 5. One of the free hydrogen atoms of ammonium cation (H4) gets coordination with un-ionized HCl molecule from the Cl1 side (e.g., see Figure 5). Then, the un-ionized HCl molecule gives the proton to the other chlorine ion. The proton is either shared between two chlorine ions,  $\text{Cl}^-\cdots\text{H}^+\cdots\text{Cl}^-$  (see for example the 1710 fs snapshot, Figure 5) or reside on one (such as the 2390 and 4000 fs snapshots, Figure 5).

One could withdraw some information from this trajectory: first of all, it is very interesting that the  $\text{NH}_3$  molecule cannot promote proton transfer from one Cl to another. On the other hand,  $\text{NH}_4^+$  catalyzes the transfer. Furthermore,  $\text{NH}_4^+$  ion wants to be solvated from all sides and tries to get more coordination, as was observed with the cluster that was mentioned above.

**$(\text{HCl})_2\cdots(\text{NH}_3)_3$  Cluster.** The cluster contains one HCl inserted into the  $\text{NH}_3$  ring and ionized. The other HCl molecule is solvating this ionized HCl molecule as shown in Figure 2c. The trajectory was run for 4 ps at an average temperature of 120 K. During the trajectory, the proton is localized on ammonium cation and the ring structure is confined. One of protons of the  $\text{NH}_4^+$  cation also makes the coordination time to time with this extra solvating HCl molecule (H11Cl2). When this happens, the H11 proton is shared between Cl1 and Cl2 atoms. The mean H11–Cl2 distance was 1.397 Å (SD = 0.179 Å), and the corresponding MP2 value was 1.362 Å. The average NH bond distances in the  $\text{NH}_4^+$  cation were 1.087 Å (SD = 0.135 Å) for N1H1, 1.082 Å (SD = 0.129 Å) for N1H2, 1.026 Å (SD = 0.073 Å) for N1H3, and 1.031 Å (SD = 0.085 Å) for N1H4. The calculated MP2 values were 1.069, 1.065, 1.019, and 1.024 Å, respectively.

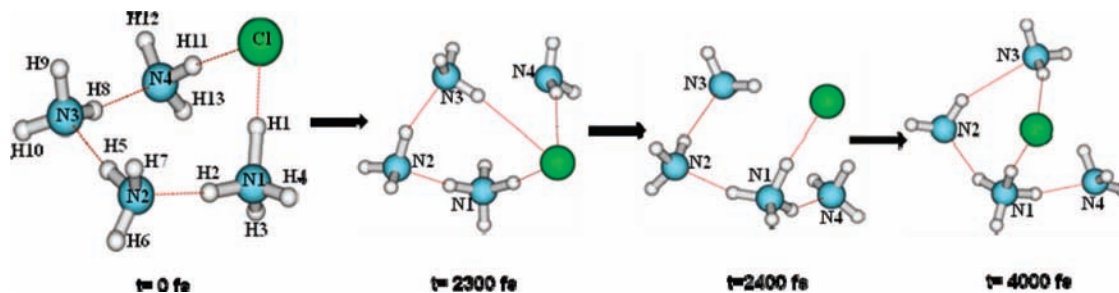


Figure 3. Snapshots from the trajectory of ammonia tetramer interacting with HCl molecule  $\text{HCl}\cdots(\text{NH}_3)_4$ .

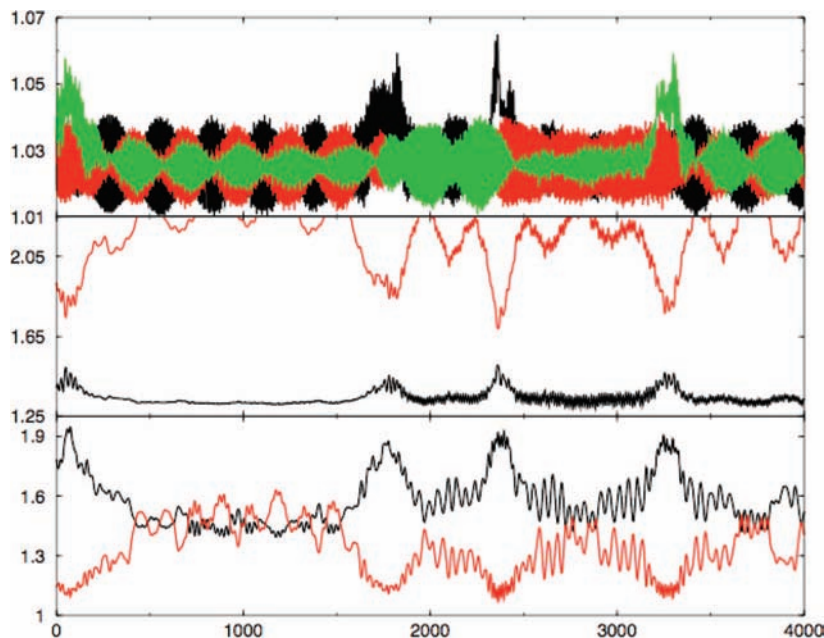


Figure 4. Time evolution of bond lengths of ammonia (top: free NH, gray; NH<sub>2</sub>, black), time evolution of distances between atoms H5 and Cl2 (middle), and time evolution of distances between atoms (H1–N, gray line) and between atoms (H1–Cl1, black line) (bottom) for  $(\text{HCl})_2\cdots\text{NH}_3$  cluster.

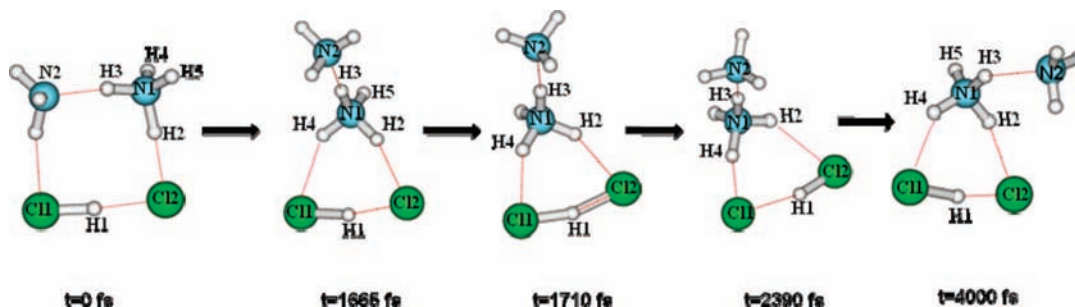


Figure 5. Snapshots from the dynamics of ammonia dimer interacting with two HCl molecules:  $\text{HCl}\cdots\text{Cl}^-\cdots\text{NH}_4^+\cdots\text{NH}_3$ .

The mean NH bond length connecting to the NH<sub>3</sub> molecule (i.e., N2H5) was 1.042 Å (SD = 0.064 Å) and that connecting to Cl<sup>-</sup> (i.e., N3H8) was 1.031 Å (SD = 0.091 Å). MP2 calculations gave a similar trend (1.034 versus 1.026 Å, respectively). The average free NH bond lengths were 1.025 Å from trajectory and 1.020 Å from MP2 level calculations.

**3.2. IR Spectra of the Clusters: Results of the Molecular Dynamics and *ab Initio* Calculations.** Before we start to discuss the spectra, we will look in Table 1 in which the energetics of the clusters is presented. From molecular dynamics it can be qualitatively estimated which structures seem to be stable, by observing geometrical preferences of the system in time. The molecular dynamics coordinates of clusters near sharing points are the input data for *ab initio* calculations. These  $(\text{NH}_3)_m\cdots\text{HCl}$ ,  $m = 2-4$ , and  $(\text{NH}_3)_m\cdots(\text{HCl})_2$ ,  $m = 1-3$ ,

structures shown in Figure 1 and Figure 2 were calculated at the MP2/aug-cc-pvDZ level too. All are ionized. Calculation of CCSD(T)/aug-cc-pvDZ energies for a cluster containing two ammonia and one HCl (the smallest one) proves that an ionized form of the cluster has lower energy than a molecular one (energy difference is about 0.8 kcal/mol). This result confirms our findings that ionized forms are more stable for this and other clusters too.

Table 1 presents the results of *ab initio* calculation of the cluster's energetics (the binding energy, which contains the CP correction, the deformation errors calculated with respect to optimal geometry of monomers, the change of zero-point energy, the deformation errors, and the dissociation energy), while the Supporting Information presents their most important distances (Table SM1). A noticeable trend for deformation error values

**TABLE 2: Important Frequencies (cm<sup>-1</sup>), Infrared Intensities (km/mol) for the Complexes of HCl⋯(NH<sub>3</sub>)<sub>m</sub>, m = 2–4, and (HCl)<sub>2</sub>⋯(NH<sub>3</sub>)<sub>m</sub>, m = 1–3, Shown in Figures 1 and 2 Calculated at the MP2/aug-cc-pvDZ Level<sup>a</sup>**

system	vibration	frequency	I <sub>c</sub>	ν <sub>c</sub> –ν <sub>m</sub>	I <sub>c</sub> /I <sub>m</sub>
HCl	stretching	3036	46.5		
NH <sub>3</sub>	umbrella-like	1045	131		
	2 deg sym bend.	1649	12.7		
	sym stretch.	3481	4.2		
	2 antisym stretch.	3635	4.2		
NH <sub>4</sub> <sup>+</sup>	3 umbrella-like	1461	139.4		
	bend s	1719	0		
	sym stretch	3379	0		
	3 antisym stretch s	3534	181.7		
Cl <sup>-</sup> ⋯NH <sub>4</sub> <sup>+</sup> ⋯NH <sub>3</sub>	<i>NH<sub>4</sub> umbrella-like combined with N1–H1 stretch</i>	1155	553.5	–306	4
	<i>NH<sub>4</sub> bend</i>	1434	726.8	–285	
	<i>bend combined with N1–H1 stretch</i>	1579	1140.9		
	<i>bend combined with N1–H1 stretch</i>	1747	1073.3		
	<i>N1–H2 sym stretch</i>	3094	654.9	–285	
Cl <sup>-</sup> ⋯NH <sub>4</sub> <sup>+</sup> ⋯(NH <sub>3</sub> ) <sub>2</sub>	<i>N1–H1 sym stretch</i>	1896	3422.6	–1483	
	<i>N1–H2 sym stretch</i>	2928	1098.6	–451	6
	sym stretch [mainly N2–H5]	3312	325.4	–169	77
	sym stretch of N3 ammonia	3394	240.9	–87	57
Cl <sup>-</sup> ⋯NH <sub>4</sub> <sup>+</sup> ⋯(NH <sub>3</sub> ) <sub>3</sub>	<i>N1–H1 antisym stretch</i>	2588	1664.8	–946	9
	<i>N1–H2 sym stretch</i>	2994	853.5	–385	
	<i>N1–H4 antisym stretch</i>	3203	642.3	–331	4
	N2–H5 stretch	3306	350.7	–175	83
	N3–H8 stretch	3366	295.8	–115	70
HCl⋯Cl <sup>-</sup> ⋯NH <sub>4</sub> <sup>+</sup>	3 umbrella-like	1454	529.2	–7	3.8
	<i>stretch of N–H1 coupled with bend of the rest of H's</i>	1611	1437.9		
	<i>coupled in-phase bend. of ammonium ion H's</i>	1714	827.2		
	H5–Cl2 stretch	2255	2443.1	–781	52.6
Cl <sup>-</sup> ⋯NH <sub>4</sub> <sup>+</sup> ⋯Cl <sup>-</sup> ⋯NH <sub>4</sub> <sup>+</sup>	<i>coupled antiphase sym stretch of four N–H bonds</i>	2745	2776.1	–634	
	<i>coupled in-phase antisym stretch of four N–H bonds</i>	2789	4005.7	–745	22
HCl⋯Cl <sup>-</sup> ⋯NH <sub>4</sub> <sup>+</sup> ⋯NH <sub>3</sub>	<i>stretch of H5–Cl2 and antiphase N1–H1</i>	2075	2463.5		
	<i>stretch of N1–H1 and in-phase H5–Cl2</i>	2322	2881.8		
	<i>sym stretch of N1–H2</i>	2836	1364.8	–543	
HCl⋯Cl <sup>-</sup> ⋯NH <sub>4</sub> <sup>+</sup> ⋯(NH <sub>3</sub> ) <sub>2</sub>	H11–Cl2 stretch	1997	2298.7	–1039	50
	<i>antisym stretch of N1–H2 and N1–H1</i>	2721	2011.3	–813	11
	<i>sym stretch of N1–H2 and N1–H1</i>	2760	1018.3	–619	
	stretch of N2–H5	3287	422.5	–194	100

<sup>a</sup> Italics indicate the results for/with respect to ammonium ion.

obtained for clusters with one and two HCl is in agreement with what was expected from the changes of geometry. As the cluster is getting bigger, new interactions are stabilizing the structures.

We have two sets of frequency results: anharmonic spectra obtained from Fourier transform of the dipole–dipole correlation function, which are illustrated in Figure 6a,b, and the results of harmonic frequencies and IR intensities calculated at MP2/aug-cc-pvDZ for optimized structures (Figures 1 and 2), which are presented in Table 2 together with the changes in the parameters caused by formation of the complexes—the shifts of the intramolecular frequencies and the ratios of IR intensities with respect to monomer values.

In contrast to ab initio normal-mode analysis, spectral calculations employing on-the-fly dipole–dipole correlation functions can reproduce broad bands and underlying continua resulting from anharmonic dynamics (Figure 6a,b). It is seen that the acid proton of HCl undergoes large-amplitude fluctuation between N1 and Cl. One can ask whether these results correspond to proton sharing between N1 and Cl atoms. The proton sharing description seems more appropriate in the case of trimers HCl⋯(NH<sub>3</sub>)<sub>2</sub> and (HCl)<sub>2</sub>⋯NH<sub>3</sub>, because of the large-amplitude fluctuations of the proton between N1 and Cl. This transient proton sharing (i.e., H<sub>3</sub>N⋯H<sup>+</sup>⋯Cl<sup>-</sup>) interpretation is supported by an intense band below 1000 cm<sup>-1</sup> of N1H1 vibration. Since the proton dynamics reflects the evolving local structures, this proton displays a modest continuum contribution

on smaller intensity in other clusters too. The average N1H1 bonds interacting with Cl atom became shorter in the series of trimer, tetramer, and pentamer, so the band frequencies are blue-shifted.

However, in larger clusters HCl⋯(NH<sub>3</sub>)<sub>3</sub> and (HCl)<sub>2</sub>⋯(NH<sub>3</sub>)<sub>3</sub> the protons are localized on ammonium units rather than fluxional, as is also evidenced by the absence of a distinct, underlying continuum in the calculated spectrum in Figure 6a,b. Such a localized proton sharing with an intense broad band at around 1000 cm<sup>-1</sup> was also observed in other systems, such as CH<sub>3</sub>OH⋯H<sup>+</sup>⋯Cl<sup>-</sup>.<sup>15,18,19</sup>

The broad bands at ca. 1500 cm<sup>-1</sup> are assigned to bending of NH<sub>4</sub><sup>+</sup>. The high-frequency end of the spectrum at 2500–3500 cm<sup>-1</sup> is dominated by the NH stretching modes (Figure 6a,b).

One may compare the above spectra to the ones obtained from normal-mode analysis of structures, employing the MP2/aug-cc-pvDZ method. In the low-energy region the ammonia molecule is characterized by rotation, bending, and umbrella-like modes. However, one may note a discrepancy between the shared-proton band obtained in on-the-fly dynamics spectra at 1000 cm<sup>-1</sup> and the corresponding, harmonic normal-mode analysis. Except the region of 1000 cm<sup>-1</sup>, the most interesting for comparison are the modes connecting with the stretching region of ammonium ion (see Table 2 and Figure 6). The spectrum of trimer has two major signals in the region above 3000 cm<sup>-1</sup>. The one at ca. 3300 cm<sup>-1</sup> mostly belong to the stretching of the ammonia nitrogen bond with hydrogen

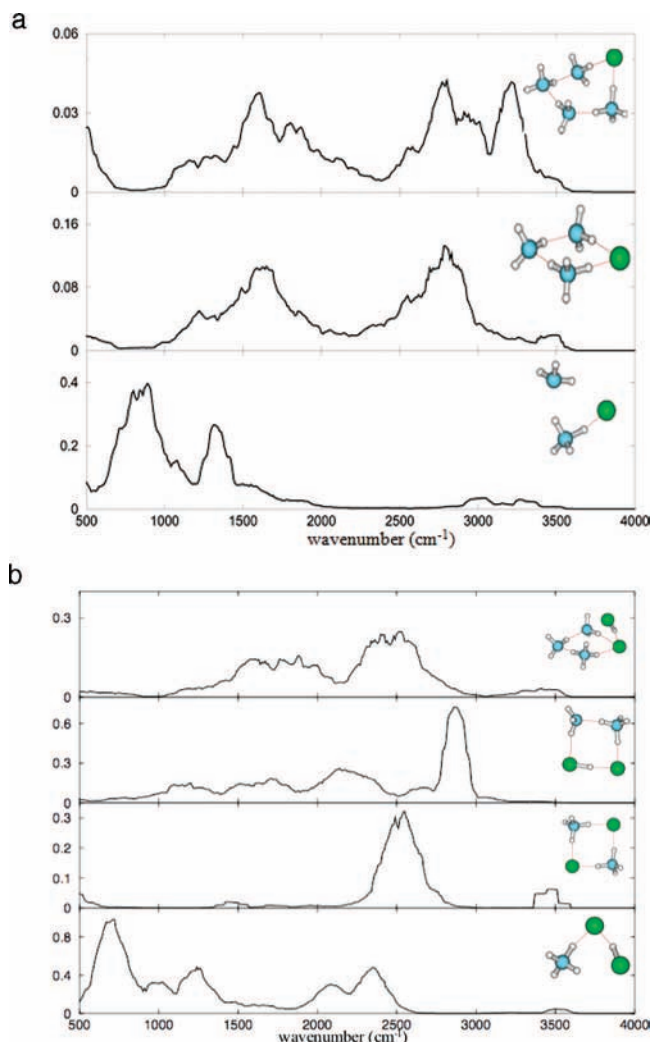


**Figure 6.** Calculated spectra from on-the-fly MD simulated trajectories of (a)  $\text{HCl}\cdots(\text{NH}_3)_m$ ,  $m = 2-4$  complexes, and (b)  $(\text{HCl})_2\cdots(\text{NH}_3)_m$ ,  $m = 1-3$  complexes. The same relative intensity units are used in all calculations. The inserted structures are also shown in Figures 1a–c and 2a–c.

interacting with chlorine anion. The one at  $3094\text{ cm}^{-1}$  belongs to the NH stretching of ammonium ion involved in formation of a hydrogen bond with the ammonia molecule (shifted with respect to ammonium ion  $-285\text{ cm}^{-1}$ ), while the NH stretching of  $\text{NH}_4^+$  interacting with chlorine ion gives a very intensive band shifted to lower frequency at ca.  $1747\text{ cm}^{-1}$ .

The spectrum of tetramer  $\text{Cl}^-\cdots\text{NH}_4^+\cdots(\text{NH}_3)_2$  is quite similar to the aforementioned one. In the region of stretching of the NH bond, the highest in energy are the signals from the NH bonds not involved in the interactions (shifted by  $-87\text{ cm}^{-1}$  with respect to ammonia monomer), then with the N1H2 bond involved in hydrogen bond with another ammonia via a hydrogen bond at  $2928\text{ cm}^{-1}$  (shifted with respect to ammonium ion by  $-451\text{ cm}^{-1}$ ) and then the N1H1 bond from ammonium ion interacting with chlorine ion at  $1896\text{ cm}^{-1}$  (shifted with respect to ammonium ion by  $-1483\text{ cm}^{-1}$ ). That means that stronger hydrogen bonds are being formed in the neighborhood of the ammonia ion in this case in comparison with the trimer. That is simply because there is a chain of ammonia connected by two hydrogen bonds, which forms more stable configuration than one hydrogen bond in the trimer. About  $1600\text{ cm}^{-1}$  there is a region of high-intensity absorption by bending modes and around  $1200\text{ cm}^{-1}$  a band from proton sharing states.

One dominant intensity signal at  $2588\text{ cm}^{-1}$  in the pentamer (Figure 1c) spectrum belongs to the N1H1 stretching bond (shifted by  $-946\text{ cm}^{-1}$  with respect to ammonium ion) interacting with the chlorine ion, while the second NH mode toward the ammonia molecule have the value of  $2994\text{ cm}^{-1}$  (shifted by  $-385\text{ cm}^{-1}$ ). Because the ammonium ion in the pentamer is a donor to three hydrogen bonds, the H-bonds formed by it are strongest, so their frequencies are lowest and intensities highest. In the set of three complexes (Figure 1a–c) the frequency values of the NH mode of ammonium ion interacting with chlorine ion increase from the trimer to pentamer and this increase correlates with the decrease of the NH length (from  $1.150$  to  $1.079\text{ \AA}$ ). On the other hand, the N1H2-type bond became longer in the series from trimer to pentamer, so the NH frequency connected with this mode is shifted to the lower values.

The trajectory spectrum of ammonia interacting with two HCl molecules has significant intensity at ca.  $2000-2450\text{ cm}^{-1}$  corresponding to H5Cl2 stretching modes ( $2255\text{ cm}^{-1}$  at harmonic spectrum). At  $1200-1400\text{ cm}^{-1}$  one can observe a band connected with bending modes of ammonium ion ( $1454\text{ cm}^{-1}$  at harmonic spectrum), and around  $1000\text{ cm}^{-1}$  there is an intensive band connected with proton sharing states.

Ammonium dimer (Figure 2b) interacting with two HCl molecules has a very simple spectrum, containing two very intensive  $2745$  and  $2789\text{ cm}^{-1}$  bands which are connected with the stretching of ammonium ion NH bonds; on the trajectory spectrum they are situated at ca.  $2500\text{ cm}^{-1}$ . On the trajectory spectrum there is also another band at ca.  $3500\text{ cm}^{-1}$  connected with NH stretching modes. The second dimer configuration (Figure 2b') has a harmonic spectrum with three intensive bands. One at  $2836\text{ cm}^{-1}$  is a stretching of the ammonium ion NH bond donating the proton to a hydrogen bond with the second ammonia molecule, while two others at  $2322$  and  $2075\text{ cm}^{-1}$  are connected with coupled stretchings of N1H1 and H5Cl2 bonds. That is in agreement with general features of the trajectory spectrum, which has a high-intensity band in the region of  $2800-2950\text{ cm}^{-1}$  and a lower one at  $2000-2400$  and  $1500-2000\text{ cm}^{-1}$ .

The structure presented at Figure 2c is similar to the structure of Figure 1b, which have an extra HCl molecule. The strongest band at  $1997\text{ cm}^{-1}$  belongs to the HCl stretching mode, shifted by  $-1039\text{ cm}^{-1}$  from its monomer value. The question can be asked concerning the extent of the changes of the  $\nu(\text{NH})$  frequency with respect to these parameters at the Figure 1b structure. Two bands in  $(\text{NH}_3)_3\cdots(\text{HCl})_2$ ,  $2721$  and  $2769\text{ cm}^{-1}$ , asymmetrical and symmetrical stretching of NH ammonium ion bonds N1H2  $\mp$  N1H1, respectively, are shifted to higher value in comparison to the Figure 1b structure ( $\nu = 1896\text{ cm}^{-1}$ ), which correlate well with the bond lengths ( $r(\text{N1H1}) = 1.066$  in Figure 2b', while  $r(\text{N1H1}) = 1.125\text{ \AA}$  in Figure 1b). Moreover, the N1 $\cdots$ N2 distance ( $2.785\text{ \AA}$ ) in this structure is much shorter than in other ones (for instance  $2.840$  in Figure 1b and  $2.895\text{ \AA}$  in Figure 1c), which could mean that in this situation second ammonia is very close to the sharing state with ammonium ion.

#### 4. Conclusions

Acid solvation of ammonia in the solid phase has been studied by MD simulations and ab initio method. On-the-fly study enables investigations of cluster dynamics in addition to minima. This model was used as a representation of a small part of the condensed-phase system, since condensed ammonia tends to be dominated by molecular rings and chains, and therefore it offers the opportunity to find a range of potentially well-defined

solvating possibilities and to study proton transfer from HCl to ammonia molecule induced in this system. The cluster models studied by us are solid in the sense that heavy atoms do not change places on the time scale of the simulations. The ab initio calculations were carried out on various acid–ammonia clusters. Our results can be summarized as follows:

(1) CP trajectories of several small ammonia clusters interacting with one or two HCl molecules were calculated. Ionization of HCl and/or sharing of the proton was observed in all complexes. Two Zundel-type ions were observed—one with proton being shared between ammonium ion and  $\text{Cl}^-$  anion ( $\text{Cl}^- \cdots \text{H}^+ \cdots \text{NH}_3$ ) in all complexes, and the second, between hydrogen chloride and  $\text{Cl}^-$  anion in  $\text{HCl} \cdots \text{Cl}^- \cdots \text{NH}_4^+ \cdots \text{NH}_3$  (Figure 2b', Figure 5) and in  $\text{HCl} \cdots \text{Cl}^- \cdots \text{NH}_4^+ \cdots (\text{NH}_3)_2$  (Figure 2c) complexes.

(2) In trimers, such as  $(\text{HCl})_2 \cdots \text{NH}_3$  and  $\text{HCl} \cdots (\text{NH}_3)_2$  clusters: although the optimized structures give ionized HCl, the proton is not localized on ammonium cation; rather it is shared between Cl and N atom.

(3) The second Zundel-type ion  $\text{HCl} \cdots \text{H}^+ \cdots \text{Cl}^-$  in  $\text{HCl} \cdots \text{Cl}^- \cdots \text{NH}_4^+ \cdots (\text{NH}_3)_2$  cluster is observed: here it is ammonium cation not  $\text{NH}_3$  molecule which catalyzes the proton transfer from HCl molecule to  $\text{Cl}^-$  ion.

(4) Structures close to the proton transfer obtained in MD calculations were the input data for ab initio calculations. All optimized at MP2/aug-cc-pvDZ level complexes are ionized. Most important for the stability of the system is the formation of a maximal number of hydrogen bonds by ammonium ion. The formation of ringlike networks of hydrogen bonds between the ammonia is also important but has lower stabilizing effect.

(5) However, at the present level of modeling, employing small clusters, the calculations confirm, in contrast to methanol clusters, that ammonia clusters are not good for the proton wire since, once the proton moves to ammonia, it is localized on the ammonium ion units.

**Acknowledgment.** This project was partly supported by SDU-BAP (Project No: 1211-m-05) and N.U.-A. is thankful for this support. P.S. and J.S. thank the Interdisciplinary Center for Computational Modeling (ICM), University of Warsaw, for providing computer time (G18-4).

**Supporting Information Available:** A table showing distances and angles between atoms in complexes  $\text{HCl} \cdots (\text{NH}_3)_m$ ,  $m = 2-4$ , and  $(\text{HCl})_2 \cdots (\text{NH}_3)_m$ ,  $m = 1-3$ . This material is available free of charge via the Internet at <http://pubs.acs.org>.

## References and Notes

- (1) Howard, N. W.; Legon, A. C. *J. Chem. Phys.* **1988**, *88*, 4694.
- (2) Legon, A. C. *Chem. Soc. Rev.* **1993**, 153, and references cited therein.

- (3) Barnes, A. J.; Beech, T. R.; Mielke, Z. *J. Chem. Soc., Faraday Trans.* **1984**, *80*, 455.
- (4) Andrews, L.; Wang, X.; Mielke, Z. *J. Am. Chem. Soc.* **2001**, *123*, 1499.
- (5) Biczysko, M.; Latajka, Z. *Chem. Phys. Lett.* **1998**, *313*, 366.
- (6) (a) Cazar, R.; Jamka, A.; Tao, F. M. *Chem. Phys. Lett.* **1998**, *287*, 549. (b) Tao, F. M. *J. Chem. Phys.* **1999**, *110*, 11121. (c) Cherg, B.; Tao, F. M. *J. Chem. Phys.* **2001**, *114*, 1720.
- (7) Snyder, J. A.; Cazar, R. A.; Jamka, A. J.; Tao, F. M. *J. Phys. Chem. A* **1999**, *103*, 7719.
- (8) Li, R. J.; Li, Z. R.; Wu, D.; Hao, X. Y.; Li, Y.; Tao, F. M.; Sun, C. C. *Chem. Phys. Lett.* **2003**, *372*, 893.
- (9) Devlin, J. P.; Farnik, M.; Suhm, M. A.; Buch, V. *J. Phys. Chem. A* **2005**, *109*, 955.
- (10) Alikhani, M. E.; Silvi, B. *PCCP* **2003**, *5*, 2494.
- (11) Kondo, M.; Kawanowa, H.; Gotoh, Y.; Sounda, R. *Surf. Sci.* **2005**, *594*, 141.
- (12) Asada, T.; Takitani, S.; Koseki, S. *J. Phys. Chem. A* **2005**, *109*, 1821.
- (13) Sorkin, A.; Dahlke, E. E.; Truhlar, D. G. *J. Chem. Theory Comput.* **2008**, *4*, 683.
- (14) Devlin, J. P.; Uras, N.; Sadlej, J.; Buch, V. *Nature* **2002**, *417*, 269.
- (15) Buch, V.; Sadlej, J.; Aytemiz-Uras, N.; Devlin, J. P. *J. Phys. Chem. A* **2002**, *106*, 9374.
- (16) Weimann, M.; Farnik, M.; Suhm, M. A. *PCCP* **2004**, *2*, 3933.
- (17) Farnik, M.; Weimann, M.; Suhm, M. A. *J. Chem. Phys.* **2003**, *118*, 10120.
- (18) Devlin, J. P.; Sadlej, J.; Hollman, M.; Buch, V. *J. Phys. Chem. A* **2004**, *108*, 2030.
- (19) Uras-Aytemiz, N.; Devlin, J. P.; Sadlej, J.; Buch, V. *J. Phys. Chem. B* **2006**, *110*, 21751.
- (20) Uras-Aytemiz, N.; Sadlej, J.; Devlin, J. P.; Buch, V. *Chem. Phys. Lett.* **2006**, *422*, 179.
- (21) Bacelo, D. E.; Fiorelli, S. E. *J. Chem. Phys.* **2003**, *119*, 11695.
- (22) Chaban, G. M.; Gerber, R. B.; Janda, K. C. *J. Phys. Chem. A* **2001**, *105*, 8332.
- (23) Zundel, G. *Adv. Chem. Phys.* **2000**, *111*, 1.
- (24) VandeVondale, J.; Krack, M.; Mohamed, F.; Parrinello, M.; Chassaing, T.; Hutter, R. *Comput. Phys. Commun.* **2005**, *167*, 103.
- (25) CP2K, <http://cp2k.berlios.de>, 2000–2004.
- (26) (a) Becke, A. D. *Phys. Rev. A* **1998**, *38*, 3098. (b) Lee, C. T.; Yang, W. T.; Parr, R. G. *Phys. Rev. B* **1988**, *37*, 785.
- (27) Goedecker, S.; Teter, M.; Hutter, J. *Phys. Rev. B* **1996**, *54*, 1703.
- (28) Buch, V.; Mohamed, F.; Parrinello, M.; Devlin, J. P. *J. Chem. Phys.* **2007**, *126*, 074503.
- (29) Devlin, J. P.; Severson, M. W.; Mohamed, F.; Sadlej, J.; Buch; Parrinello, M. *Chem. Phys. Lett.* **2005**, *408*, 439.
- (30) Buch, V.; Mohamed, F.; Krack, M.; Sadlej, J.; Devlin, J. P.; Parrinello, M. *J. Chem. Phys.* **2004**, *121*, 12135.
- (31) Buch, V.; Mohamed, F.; Parrinello, M.; Devlin, J. P. *J. Chem. Phys.* **2007**, *126*, 021102.
- (32) Dunning, T. H. *J. Chem. Phys.* **1989**, *90*, 1007.
- (33) Boys, S. F.; Bernardi, F. *Mol. Phys.* **1970**, *19*, 553.
- (34) Schmidt, M. W.; Baldrige, K. K.; Boatz, J. A.; Elbert, S. T.; Gordon, M. S.; Jansen, J. H.; Koseki, S.; Matsunaga, N.; Nguyen, K. A.; Su, S.; Windus, T. L.; Dupuis, M.; Montgomery, J. A. *J. Comput. Chem.* **1993**, *14*, 1347.
- (35) Latajka, Z.; Scheiner, S. *J. Chem. Phys.* **1987**, *10*, 5928.
- (36) Holt, J. S.; Sadoskas, D.; Pursell, Ch. J. *J. Chem. Phys.* **2004**, *120*, 7153.
- (37) Almeida, T. S.; Coutinho, K.; Cabral, B. J.; Canuto, S. *J. Chem. Phys.* **2008**, *128*, 014506.
- (38) Kulczycka, K.; Kalbarczyk, P.; Uras-Aytemiz, N.; Sadlej, J. *J. Phys. Chem.* **2008**, *112*, 3870.